NICOTINE ADDICTION DECREASES DYNAMIC CONNECTIVITY FREQUENCY IN FUNCTIONAL MAGNETIC RESONANCE IMAGING

Victor M. Vergara, PhD and Vince D Calhoun, Phd

Tri-institutional center for Translational Research in Neuroimaging and Data Science (TReNDS)
25 Park Place, Atlanta GA 30303

ABSTRACT

Abnormal functional network connectivity has been related to nicotine addiction where similar patterns of dysfunction were found after applying dynamic or static connectivity methods. Further developments indicate that connectivity patterns might also exhibit a dysfunctional frequency spectrum. This work employs a quasi-stable time-varying functional connectivity framework to explore frequency effects related to nicotine use. Results suggest that nicotine abstinence in addicted subjects is linked to a frequency decrease of resting state connectivity fluctuations. This effect was found in one out of four quasi-stable connectivity states.

Index Terms— Functional connectivity, fMRI, nicotine addiction.

1. INTRODUCTION

Allen et. al [1] described functional states as temporal lapses of functional connectivity during which the connectivity remained quasi-stable. The concept has been widely applied to whole brain analysis where the number of time-varying connectivity estimations is large. Detecting quasi-stable lapses of time is achieved using unsupervised machine learning methods such as clustering. Each cluster results in a quasi-stable functional connectivity pattern visually displayed as the cluster centroid. Centroids are estimated by the vector of average values from the members of the cluster. This way, each clustered element is associated with a given cluster resulting in a membership function. Membership values point to one of the centroids representing the connectivity pattern of the functional state.

The assumption that centroids represent the predominant pattern of each state has become useful when interpreting the clustering results. This representation agrees with the concept of quasi-stable connectivity. However, little attention has been put to the relatively small connectivity fluctuations observed within the cluster. To include information from temporal fluctuations, one method that has been proposed is to cluster a concatenation of functional connectivity and its temporal derivatives [2]. The main contribution of this method is the unveiling of a new set of cluster patterns resurfacing from the derivatives showing patient-control differences [3, 4]. The inclusion of derivatives also revealed periodicity of functional connectivity at the multivariable level that is comparable to the behavior of dynamic systems [5]. This work explores changes in oscillatory frequency linked to nicotine. The study of this oscillatory behavior exhibited by functional connectivity can lead to a better description of resting state brain activity as well as provide newer features for brain illness biomarkers.

The rest of this manuscript is organized as follows. Section 2 describes the smoker sample cohort and the methods employed in this work. Section 3 presents the main results. Section 4 discusses the observations made through the application of the methods employed.

2. METHODS

2.1. Sample Cohort

The sample cohort for this study included 80 subjects (37 females) with medium to high nicotine dependence assessed by the Fagerström Tolerance Questionnaire (FTQ). The FTQ scores ranged from 7 to 12. Smoking was avoided 3 h before scanning. Subjects age ranged from 19 to 54 with an average of 34.8 (standard deviation of 10.2). Subjects did not suffer from injury to the brain, brain-related medical problems, bipolar or psychotic disorders. A urinalysis test rejected the use of other drugs including marijuana.

2.2. Preprocessing

Resting state functional MRI data were collected on a 3T Siemens TIM Trio (Erlangen, Germany) scanner. Participants kept their eyes open during the 5-minute resting scan. Echo-planar EPI sequence images (TR = 2,000 ms, TE = 29 ms, flip angle = 75°) were acquired with an 8-channel head coil. Each volume consisted of 33 axial slices (64 × 64 matrix, 3.75 × 3.75 mm2, 3.5 mm thickness, 1 mm gap). Resting state fMRI data were preprocessed using the statistical parametric mapping software (SPM; http://www.fil.ion.ucl.ac.uk/spm) [6] including slice-timing correction, realignment, co-registration and spatial normalization. Images were transformed to the Montreal

Neurological Institute standard space. The first five scans were discarded to allow for T1 equilibration. The DVARS method [7] was used to find spike regressors where the root mean square head movement exceeded 3 standard deviations. Time courses, with a size of 145 time steps, were orthogonalized with respect to i) linear, quadratic and cubic trends; ii) the 6 realignment parameters and iii) realignment parameters derivatives. The decision to pre-process these nuisances at this point is based on recent recommendations in the field [8]. The fMRI data were smoothed using a full-width-at-half-maximum Gaussian kernel of size 6 mm. The data were then analyzed with Infomax based group independent component analysis (gICA) [9, 10] with 120 and 100 components for the first and second decomposition levels respectively [11]. A total of N=39 gICA components were selected for further analysis. Each component points to a specific brain network with a corresponding time varying signal that we denote as the time course. In this resting state experiment, each gICA component is denoted a resting state network (RSN). RSN time courses were then filtered using a band-pass filter 0.01 to 0.15 Hz.

2.3. Dynamic connectivity and derivatives

The next step was to estimate a time varying functional connectivity from RSN time courses that we called the dynamic functional network connectivity (dFNC). The dFNC data was obtained using the average-sliding-time-window-correlation (ASWC) approach [12] with nominal window (44 sec) and average (50 sec) lengths. Each subject had 98 dFNC time courses. Since the estimated ASWC data is of discrete nature, we employed discrete derivative techniques [3]. The first sample does not have a previous one, thus we utilize forward differences by subtracting the second sample from the first. Backwards difference was use for the last sample by subtracting this last one from the previous one. Any sample in the middle was processed using the central difference corresponding to the subtraction of the next sample minus the previous sample divided by two. The derivative was applied to the ASWC from each pair of RSNs. The next step in the dFNC pipeline is to apply clustering. We concatenated the ASWC and its temporal difference (estimated derivatives). For each time point there will be 741 (N(N-1)/2) ASWC values plus 741 (N(N-1)/2) derivatives. A total of 1482 (N(N-1)) values per time point were used for the clustering algorithm.

2.4. Clustering

Obtained dFNC data were clustered using the k-means clustering method with a correlation distance to obtain a finite set of dFNC states. Since the number of clusters k is a parameter that must be estimated before continuing, we used the Davies-Bouldin (DB) index to estimate the number of valid clusters as evidence suggests this is an efficient method of estimating k [13, 14]. We ran clustering with nine different values of k ranging from 2 to 10 and a DB index was estimated for each one. The optimal k is indicated in the DB index plot by its minimum shown in Figure 1 as k=6.

Following the procedure previously suggested for derivatives in [5], we looked for possible similar cluster patterns. In particular, it is possible that a single large cluster is divided in two if derivates are included in the k-means. In that case the functional connectivity patterns should be highly similar, but with different derivatives. This is the case illustrated in Figure 2, where two pairs of centroids are highly correlated and their derivatives are of opposite sign. Figure 3 shows centroids which consist of a typical dFNC pattern and an additional derivative of dFNC pattern. Due to the similarities shown in Figure 2 we grouped clusters 1 and 2 into a dynamic state denoted as State A. Clusters 3 and 4 were also grouped as State B. Clusters 5 and 6 could not be grouped and were assigned one state each.

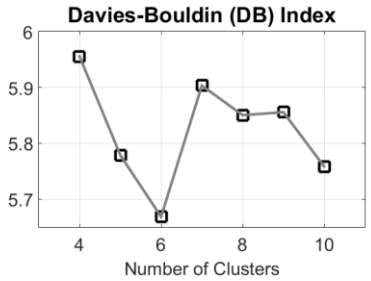

Figure 1. The optimal number of clusters was obtained using the Davies-Bouldin (DB) index. The minimum DB index points to the optimal number of clusters as 6.

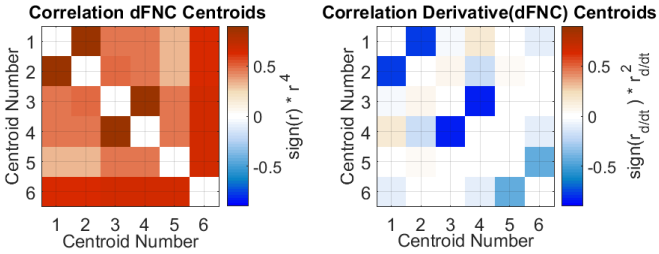

Figure 2. Clusters were paired according an opposite pattern of the derivatives. The numeric pairing is divided in two, one for the dFNC data and one for derivatives. The dFNC parts of the centroids are correlated to establish their similarity. Paired dFNCs must exhibit a strong similarity. The derivative part shows strong correlations but opposite signs. These two characteristics do not apply to centroids 5 and 6.

2.5. Oscillations

One of the main explanations for the presence of clusters with opposite sign derivatives is the existence of oscillations. For example, during a lapse of time corresponding to State A, the membership function for the corresponding time will oscillate between cluster 1 and cluster 2. A similar example could be made of State B with clusters 3 and 4. Figure 4 show a single time course example for the two cases we described. Even though not all subjects

show the same periodic patterns, the oscillations in Figure 4 are relatively common and easy to find through dFNC data.

For each state where oscillations exist (states A and B), we find the frequency with highest power. The frequency with maximum power in the example of Figure 4 corresponds only to the left angular gyrus versus supplementary motor area. We repeated the same procedure for all 741 pairs of brain areas, averaged the frequency power spectrum and found the frequency with the maximum power for each subject. Note that in order to achieve for a given subjects, the corresponding membership function must include clusters 1 and 2. For this reason, not all subjects participated on the analysis of every state. Finally, we correlate the maximum frequency the FTQ score.

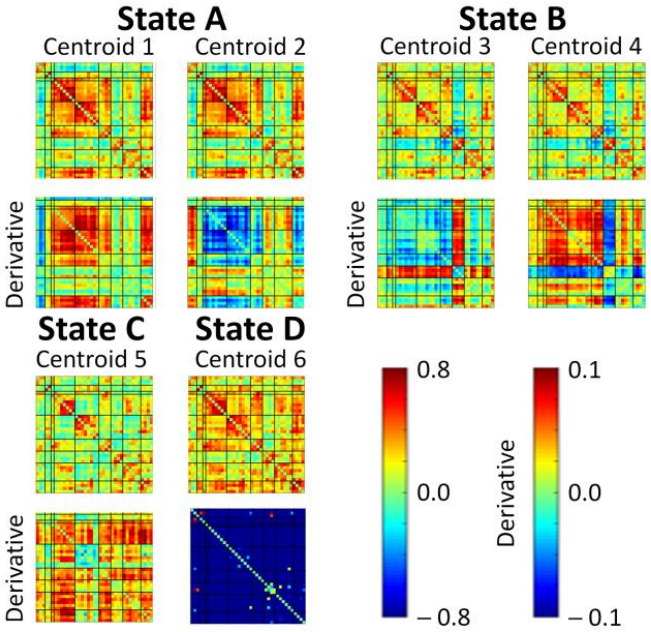

Figure 3. Centroids for the k=6 k-mean clustering. Clusters with similar characteristics (see Figure 2) were grouped in four states: A, B, C and D. States A and B include two clusters each.

3. RESULTS

We performed a dwell time analysis for each cluster. The mean dwell time for all six clusters are [15.0, 17.3, 17.4, 17.8, 12.7, 19.8] % for each cluster in order from 1 to 6. In this case, if a subject did not dwell in a given cluster then the estimation was set to zero. We obtained dwell times for each subject and correlated with the FTQ score without having a significant p-value.

The next analysis focused on states instead of clusters. In this case we were looking for contiguous lapses of time where the same state is detected establishing a quasi-stable condition. Thus, only lapses of a stable state of 60 min or larger were allowed. States [A, B, C, D] had mean occupancy rates of [20.7, 21.8, 7.4, 7.2] % and none of the correlations with FTQ was significant.

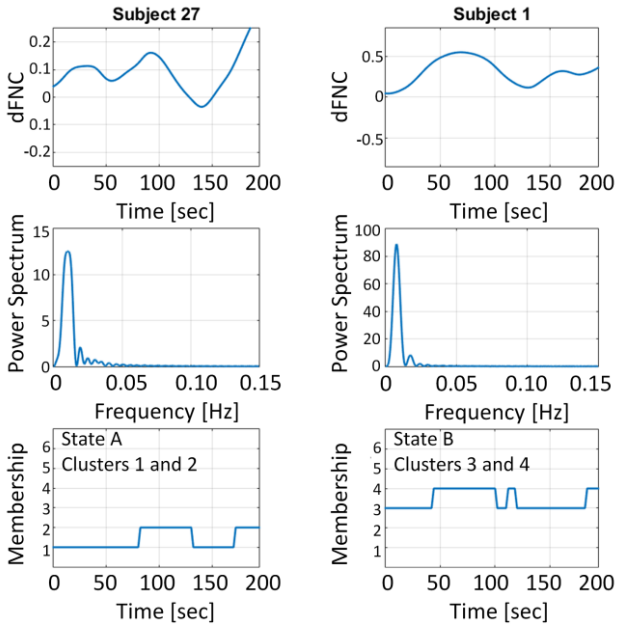

Figure 4. Examples of oscillatory behavior observed in the dFNC time course and reflected in the k-means membership. The time course corresponds to the ASWC between the left angular gyrus and the supplementary motor area.

The last result was to correlate the main frequency, that where the frequency power spectrum achieved maximum value, with nicotine addiction. The correlations for the each state were [0.02, –0.42, –0.18, –0.13] where State B exhibit a significant correlation with p-value < 0.05. The correlation result is illustrated in Figure 5.

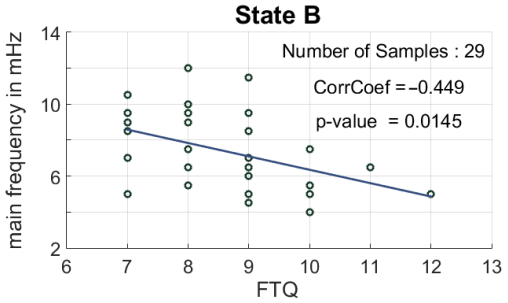

Figure 5. Correlation between main frequency (millihertz) and nicotine addiction measured. Significant correlation was found in State B.

4. DISCUSSION

This work analyzed dynamic characteristics of dFNC from nicotine addiction subjects based on the frequency exhibited by different dFNC states. Quasi-stable functional states were acquired extending the concept of stability to allow for a quasi-stable oscillation within the time lapse a state last. While dwell time and occupancy rate measurements showed no relationship with addiction behavior, frequency analysis of these oscillations reveals a relationship between nicotine addiction and the oscillatory frequency.

Previous studies in functional connectivity have found focalized connectivity changes pinpointing specific brain regions. Connectivity decreased between thalamus and putamen while increased within the default mode network (DMN) [15]. Several studies support the effect of nicotine on the DMN [16]. With respect to subcortical regions, the putamen was also an area related to nicotine addiction in dFNC [17]. Those dFNC results also showed that effects can be specific to a single dFNC state.

Previous functional connectivity studies relied on differences between correlation strength. For this reason it difficult to compare results shown here with previous studies in fMRI. To the best knowledge of the authors, this is the first time the frequency of dynamic functional fluctuations within a dFNC state have been found to be related to nicotine addiction. Parallel evidence for the frequency reduction linked to nicotine has been reported for electroencephalogram data. Nicotine abstinence increases the power of the lower theta frequency when compared to higher alpha and beta frequencies [18]. Other studies show that nicotine administration causes a shift towards alpha frequencies [19]. It is possible that the 3 h abstinence period of the smokers started a shift towards lower frequencies reflected in the negative correlation between FTQ and main frequency from State B.

5. ACKNOWLEDGEMENTS

This work was supported by grants from the National Institutes of Health grant numbers 2R01EB005846, R01REB020407, and P20GM103472; and the National Science Foundation (NSF) grants 1539067/1631819 to VDC.

12. REFERENCES

[1] E. A. Allen, E. Damaraju, S. M. Plis, E. B. Erhardt, T. Eichele, and V. D. Calhoun, "Tracking whole-brain connectivity dynamics in the resting state," Cereb Cortex, vol. 24, pp. 663-76, Mar 2014.

[2] F. Espinoza, E. Damaraju, V. Vergara, K. Henke, J. Turner, and V. Calhoun, "Characterizing whole brain temporal variation of functional connectivity via zero and first order derivatives of sliding window correlations," presented at the Sixth Biennial Conference on Resting State and Brain Connectivity, 2018.

[3] F. A. Espinoza, V. M. Vergara, E. Damaraju, K. G. Henke, A. Faghiri, J. A. Turner, et al., "Characterizing Whole Brain Temporal Variation of Functional Connectivity via Zero and First Order Derivatives of Sliding Window Correlations," Frontiers in Neuroscience, vol. 13, 2019.

[4] H. J. van der Horn, V. M. Vergara, F. A. Espinoza, V. D. Calhoun, A. R. Mayer, and J. van der Naalt, "Functional outcome is tied to dynamic brain states after mild to moderate traumatic brain injury," Hum Brain Mapp, Oct 21 2019.

[5] V. M. Vergara, H. J. van der Horn, A. R. Mayer, F. A. Espinoza, J. van der Naalt, and V. D. Calhoun, "Mild Traumatic Brain Injury Disrupts Functional Dynamic Attractors of Healthy Mental States," ed, 2019.

[6] K. J. Friston, "Statistical parametric mapping," in Neuroscience Databases, ed: Springer, 2003, pp. 237-250.

[7] J. D. Power, K. A. Barnes, A. Z. Snyder, B. L. Schlaggar, and S. E. Petersen, "Spurious but systematic correlations in functional connectivity MRI networks arise from subject motion," Neuroimage, vol. 59, pp. 2142-2154, 2012.

[8] V. M. Vergara, A. R. Mayer, E. Damaraju, K. Hutchison, and V. D. Calhoun, "The effect of preprocessing pipelines in subject classification and detection of abnormal resting state functional network connectivity using group ICA," Neuroimage, vol. 145, pp. 365-376, Jan 15 2017.

[9] V. Calhoun, T. Adali, G. Pearlson, and J. Pekar, "A method for making group inferences from functional MRI data using independent component analysis," Human brain mapping, vol. 14, pp. 140-151, 2001.

[10] V. D. Calhoun and T. Adali, "Multisubject independent component analysis of fMRI: a decade of intrinsic networks, default mode, and neurodiagnostic discovery," IEEE Rev Biomed Eng, vol. 5, pp. 60-73, 2012.

[11] E. B. Erhardt, S. Rachakonda, E. J. Bedrick, E. A. Allen, T. Adali, and V. D. Calhoun, "Comparison of multi-subject ICA methods for analysis of fMRI data," Hum Brain Mapp, vol. 32, pp. 2075-95, Dec 2011.

[12] V. M. Vergara, A. Abrol, and V. D. Calhoun, "An average sliding window correlation method for dynamic functional connectivity," Hum Brain Mapp, Jan 19 2019.

[13] A. Abrol, V.M. Vergara, F.A. Espinoza, V.D. Calhoun, "Selection of Efficient Clustering Index to Estimate the Number of Dynamic Brain States from Functional Network Connectivity," presented at the EMBC, 2019.

[14] V. M. Vergara, M. Salman, A. Abrol, F. A. Espinoza, and V. D. Calhoun, "Determining the Number of States in Dynamic Functional Connectivity Using Cluster Validity Indexes," Journal of Neuroscience Methods, p. 108651, 2020.

[15] V. M. Vergara, J. Liu, E. D. Claus, K. Hutchison, and V. Calhoun, "Alterations of resting state functional network connectivity in the brain of nicotine and alcohol users," Neuroimage, vol. 151, pp. 45-54, May 1 2017.

[16] M. T. Sutherland, M. J. McHugh, V. Pariyadath, and E. A. Stein, "Resting state functional connectivity in addiction: Lessons learned and a road ahead," Neuroimage, vol. 62, pp. 2281-95, Oct 01 2012.

[17] V. M. Vergara, B. J. Weiland, K. E. Hutchison, and V. D. Calhoun, "The Impact of Combinations of Alcohol, Nicotine, and Cannabis on Dynamic Brain Connectivity," Neuropsychopharmacology, vol. 43, pp. 877-890, Mar 2018.

[18] W. B. Pickworth, R. I. Herning, and J. E. Henningfield, "Spontaneous EEG changes during tobacco abstinence and nicotine substitution in human volunteers," J Pharmacol Exp Ther, vol. 251, pp. 976-82, Dec 1989.

[19] E. F. Domino, M. Riskalla, Z. Yingfan, and E. Kim, "Effects of tobacco smoking on the topographic eeg II," Progress in Neuro-Psychopharmacology and Biological Psychiatry, vol. 16, pp. 463-482, 1992.